

Sensor and Simulation Notes

Note 578

12 September 2017

Micro-Impulse Radiating Antenna (MIRA)

D.V. Giri

Pro-Tech, 11-C Orchard Court, Alamo, CA 94507

Dept. of ECE, University of New Mexico, Albuquerque, NM 87130

Abstract

In this note, we describe the electromagnetic design considerations of a small (perhaps the world's smallest) or Micro-Impulse Radiating Antenna (MIRA). This author had designed, analyzed, fabricated and tested a 3.66 m diameter IRA (perhaps the world's largest) in 1994 [1-3]. This very first IRA was called the Prototype IRA. We are presenting the design of a Micro-IRA with a diameter of 5 cm for future applications in the areas of detection of hidden objects of cm sizes. At this point, the exclusive interest is in design and analysis of this Micro-IRA.

Contents

Section		Page
1	Introduction	3
2	Transient Source Considerations.	3
3	Near, Intermediate and Far fields.	9
4	Fabrication Considerations	12
5	Summary	18
	References	18

Acknowledgment

I am thankful to Prof. Yanzhao Xie, of Xi'an Jiaotong University for suggesting this problem.

1. Introduction

An Impulse Radiating Antenna (IRA) is a paraboloidal reflector fed by a pair of coplanar conical transmission lines. Each transmission line has a characteristic impedance of 400 Ohms. The net antenna impedance is 200 Ohms when the two feed lines are connected in parallel. The first one built circa 1995 was called the Prototype IRA and had a diameter of 3.66 m. Many IRAs have been built since, and there have been variations on the original theme as well. The objective of this note is to design and analyze a very small IRA with a diameter of 5 cm.

2. Transient Source Considerations

The [diameter D/speed of light c] needs to be much larger than the rise time of the excitation pulse. In other words, need many rise times in the diameter. Or $[D/(c t_r)]$ should be $\gg 1$. If the diameter is 5 cm, this corresponds to a time of travel of 166 ps. Consequently, we should use a pulse source whose risetime is small compared to 166 ps.

We find PSPL 4015 [4] could be useful at least for initial modelling.

The advertised output has the following specifications.

Voltage amplitude = - 9 V

Fall time at the beginning of the transient waveform = 15 ps

Pulse duration = 10 ns

Rise time at the end of the pulse = 250 ps

$[D/(c t_r)] = [166 \text{ ps}/15 \text{ ps}] = 11$. That means 11 rise times in the diameter, which is a good number.

The output of the transient pulse is of the box car type [Appendix B; Waveform 17 in 3] and can be analytically modelled by

$$V(t) = V_0 \left[\frac{1}{1 + \exp(-\alpha_1(t - t_1))} - \frac{1}{1 + \exp(-\alpha_2(t - t_2))} \right] \quad (\text{Volts}) \quad (1)$$

In this waveform, it is possible to independently choose the “flat top” amplitude, duration, the fall time at the beginning of the pulse, and the rise time at the end of the pulse

We have chosen peak amplitude of -9V, 10-90% fall time of 15 ps, pulse duration of 10 ns and a rise time at the end of the pulse of 250 ps. In practice, it is difficult to bring the voltage back to zero from its peak, as fast as it can be taken from 0 to peak.

The voltage waveform of equation (1) has an analytical Fourier transform given by

$$\tilde{V}(\omega, \alpha_2) = \left[\frac{\pi}{\alpha_1} \operatorname{csc}\left(\frac{\pi j \omega}{\alpha_1}\right) \exp(-j \omega t_1) - \frac{\pi}{\alpha_2} \operatorname{csc}\left(\frac{\pi j \omega}{\alpha_2}\right) \exp(-j \omega t_2) \right] (\text{V} / \text{Hz}) \quad (2)$$

where $\omega = 2\pi f$ is the radian frequency.

The numerical values we have chosen are:

$$V_0 = -9V ;$$

$$\alpha_1 = 1.76 \times 10^{10} \text{ resulting in a fixed (10-90\%) rise time of 250 ps}$$

$$t_1 = 1 \text{ ns}$$

$$t_2 = 11 \text{ ns resulting in a pulse duration} = (t_2 - t_1) = 10 \text{ ns}$$

$$\alpha_2 = 2.92 \times 10^{11} \text{ resulting in a fixed (10-90\%) fall time of 15 ps}$$

The resulting time domain waveform is shown plotted in Figure 1. Figure 2 shows the details of the fall time of 15 ps at the beginning of the waveform. Figure 3 has the details of the rise time of 250 ps at the end of the waveform, and Figure 4 has the magnitude spectrum.

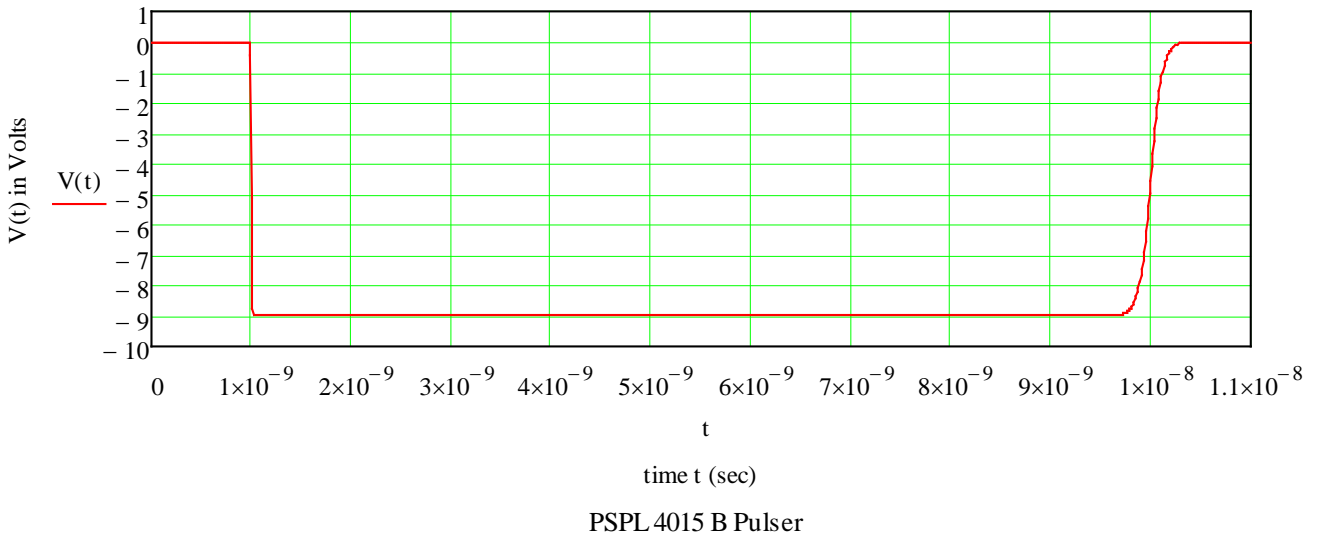


Figure 1. Modelled output of the PSPL 4015 B pulser

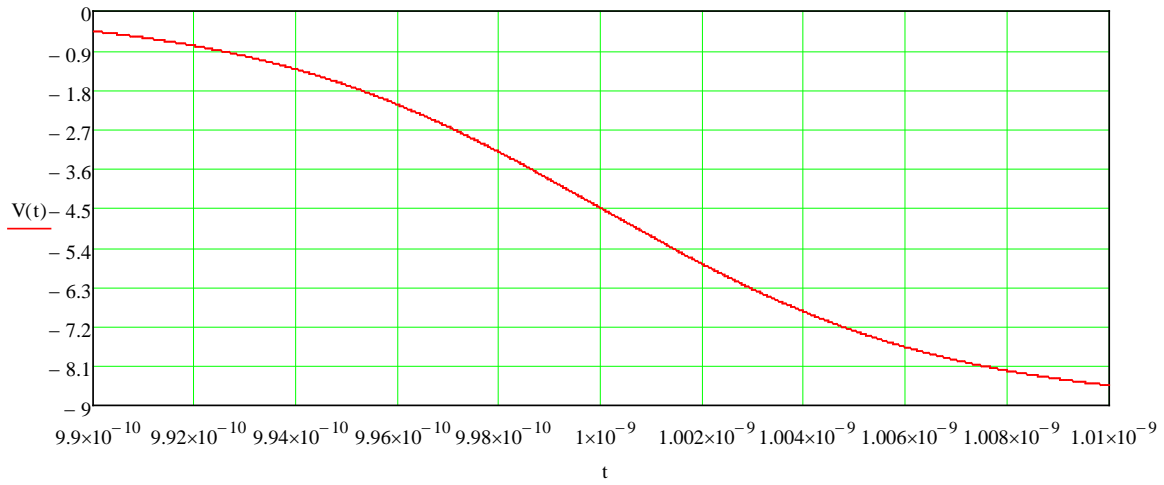


Figure 2. The fall time (15 ps) at the beginning of the transient waveform

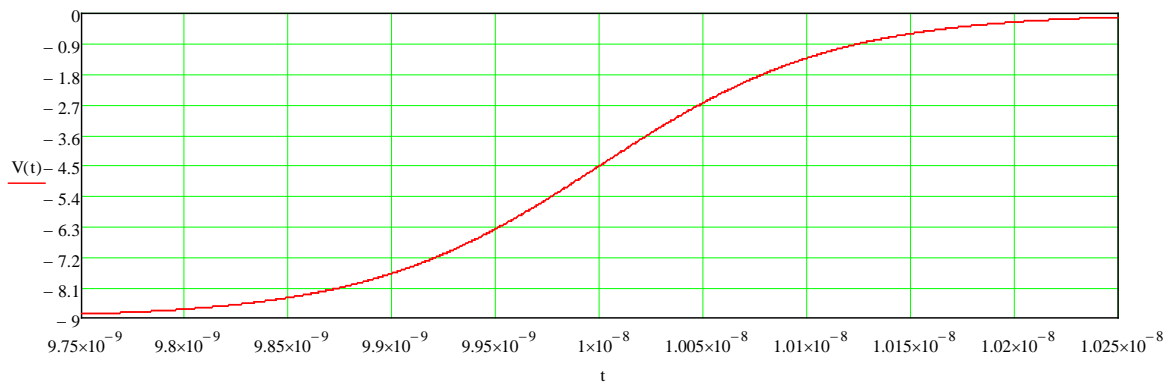


Figure 3. The rise time (250 ps) at the end of the transient waveform

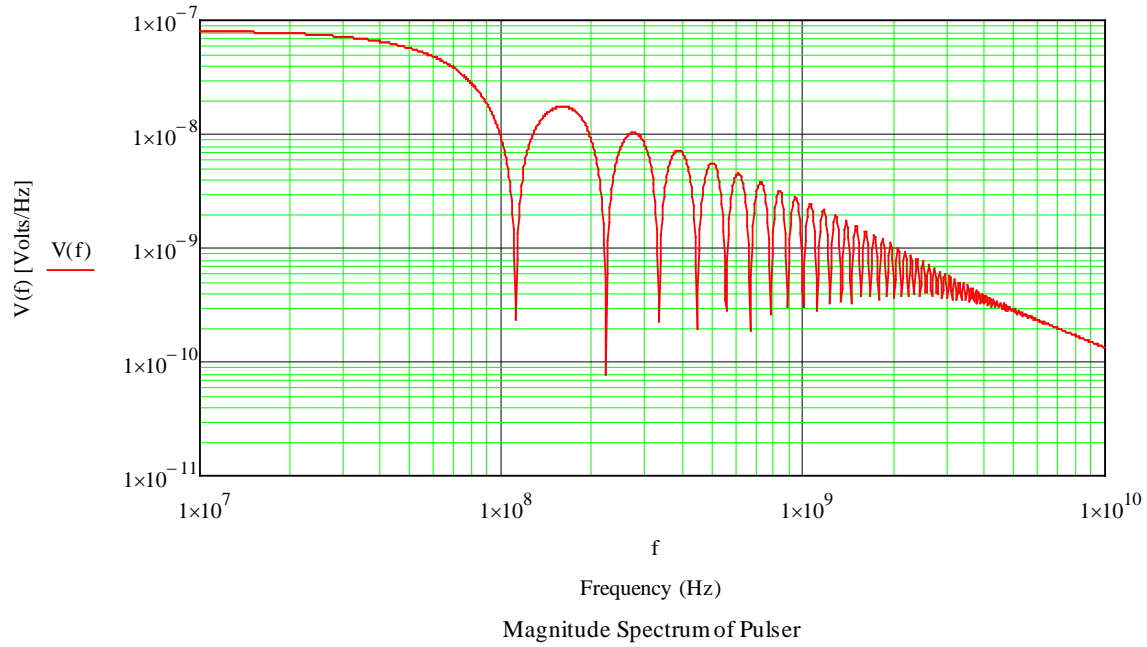


Figure 4. The magnitude spectrum of the transient waveform

It can be observed that the null frequencies in the magnitude spectrum correspond to the reciprocal of the pulse width and its harmonics.

After a careful consideration of this transient source, we have decided not to use this pulser, because of low amplitude, and also the nulls or no voltage at frequencies of approximately 100 MHz and its harmonics.

A second option for the transient source was found to be FID SP -2 offered by FID Technologies [6]. The pulse waveform is a double exponential with an amplitude of 2 kV, 10-90% rise time of 20 ps and a FWHM of 1 ns, This waveform is modeled by

$$\begin{aligned}
 V(t) = & \begin{cases} V_o (1+a) e^{-\frac{\beta t}{t_d}} \left[\left(\frac{1}{2} \right) \operatorname{erfc}(\sqrt{\pi} |t|/t_d) \right] & t < 0 \\
 V_o (1+a) e^{-\frac{\beta t}{t_d}} \left[1 - \left(\frac{1}{2} \right) \operatorname{erfc}(\sqrt{\pi} t/t_d) \right] & t > 0 \end{cases}
 \end{aligned} \tag{3}$$

$\operatorname{erfc}(z)$ is the complimentary error function given by

$$\operatorname{erfc}(z) = 1 - \operatorname{erf}(z) = \frac{2}{\sqrt{\pi}} \int_z^{\infty} \exp(-t^2) dt \quad (4)$$

$$\tilde{V}(\omega) = \frac{V_0 (1+a) t_d}{(\beta + j\omega t_d)} e^{\left[\frac{1}{4\pi} (\beta + j\omega t_d)^2 \right]} \quad (5)$$

This analytical model of the pulser is still characterized by three numbers and has continuous derivatives. This model can be explained as follows. Consider a Gaussian waveform. An integrated Gaussian is an s-shaped waveform. When this s-shaped waveform reaches its peak, we add an exponential decay factor to it. Such a process is represented by the time domain expression in (3). FID SP-2 pulser outputs are well represented by this model. The parameters are:

$$V_0 = 2 \text{ kV}, \quad \beta = 0.01425, \quad \alpha = 0.019, \quad t_d = \text{rise time} = 20 \text{ ps}$$

With the above set of constants, we will get an exponential decay time of 1.404 ns and a FWHM = 1 ns. The resulting time domain waveform is shown plotted in Figure 5. Figure 6 shows the rise portion; Figure 7 shows the derivative of this pulse waveform. Figure 8 has the magnitude spectrum.

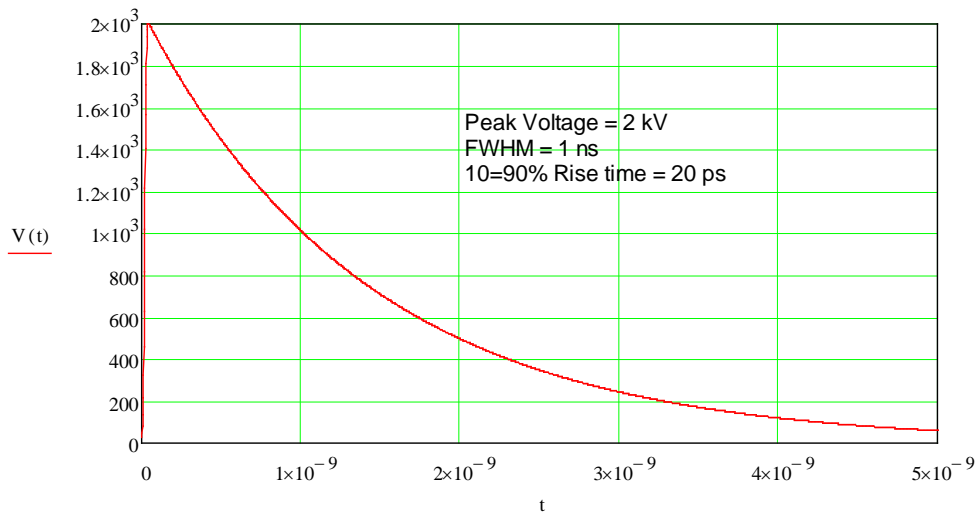


Figure 5. Modelled output of the FID SP-2pulser from FID Technologies; The peak amplitude of 2 kV and the FWHM of 1ns can be seen in this Figure.

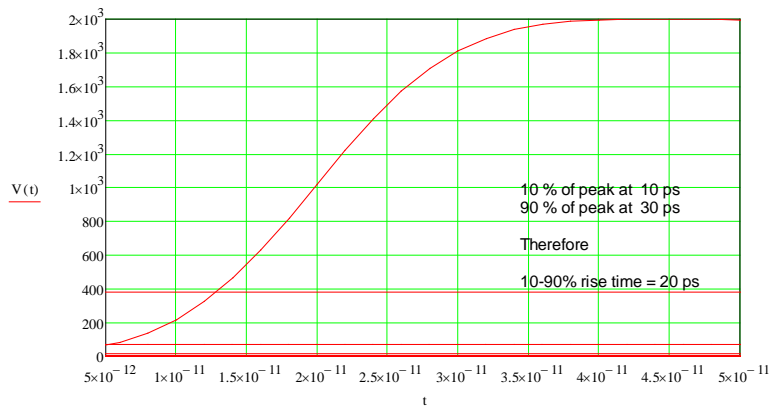


Figure 6. The rise time (20 ps) at the beginning of the transient waveform

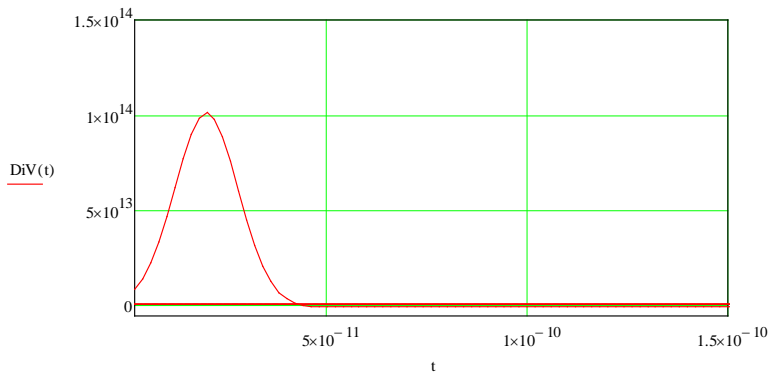


Figure 7. The time derivative of the of the transient waveform

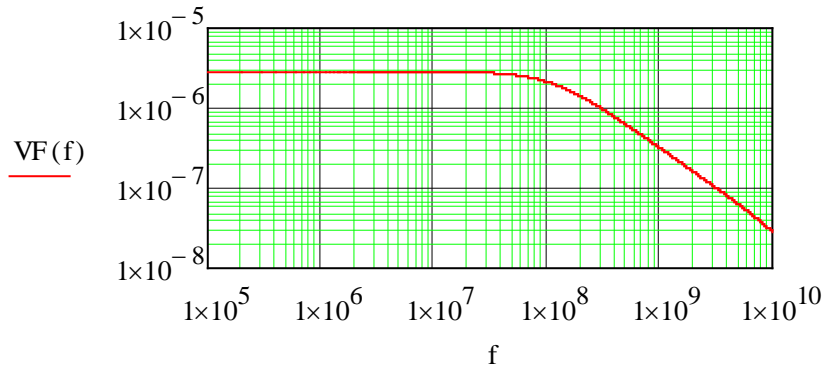


Figure 8. The magnitude spectrum [Volts/Hz] of the transient waveform of FPG SP-2 pulser

From Figure 7, we see that the peak value of the derivative of this waveform is 10^{14} V/s. This means the maximum rate of rise of this waveform is given by

$$\begin{aligned} \text{maximum rate of rise} \equiv t_{mrr} &= \frac{V_{peak}}{\left(\frac{dV}{dt}\right)_{peak}} \\ &= t_e \quad (\text{for an ideal exponential rise}) \end{aligned} \quad (6)$$

For the current pulser waveform the maximum rate of rise is given by $2 \text{ kV}/[10^{14} \text{ (V/s)}] = 20 \text{ ps}$, same as the 10-90% rise time. We also note that the far field for this antenna starts at a distance of [3]

$$\text{Far field starts at (approx.)} = [D^2 / (2 c t_r)] = (5 \text{ cm})^2 / (2 \times 3 \times 10^8 \times 20 \text{ ps}) = 20.83 \text{ cm} \quad (7)$$

3. Near, Intermediate and Far Fields

Mikheev et. al, [5] have proposed a simple method for calculating the near, intermediate and far fields of an IRA antenna. Basically, this method uses the conical transmission-line fields reflected in the parabolic mirror. If the antenna was a flat plate, the conical transmission-line would have an identical mirror image in the flat plate, resulting in the feed line and its image having the same expansion angle. However, since the antenna is paraboloidal in shape, the image is also a conical transmission line with a different expansion angle. The various geometrical parameters for boresight field calculations are shown in Figure 9.

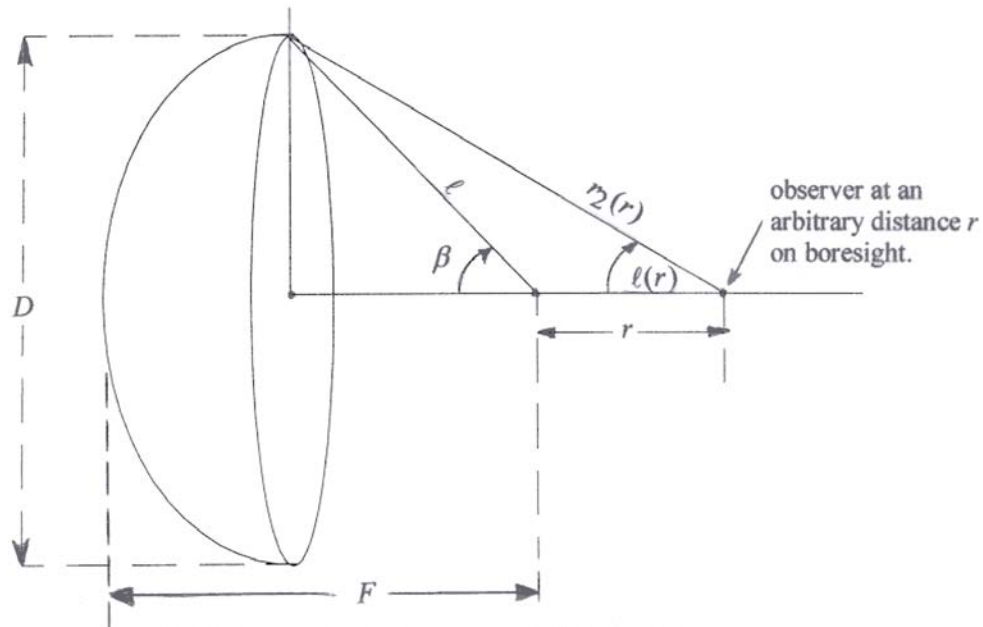


Figure 9. The geometry for boresight field calculations

The total electric field at any point on the boresight axis, at a distance of r from the focal point is given by

$$E(r,t) = -\frac{1}{2f_g\pi} \left[\begin{array}{l} \frac{V\left(t-\frac{r}{c}\right)}{r} \frac{\sin(\beta)}{1+\cos(\beta)} \\ - \frac{V\left(t-\frac{\ell}{c}-\frac{r_2}{c}\right)}{r_2} \frac{\sin(\beta)+\sin(\gamma)}{1+\cos(\beta-\gamma)} \\ - \frac{4V\left(t-\frac{2F}{c}-\frac{r}{c}\right)}{D} \\ - (2+2\cos(\gamma)) \frac{V\left(t-\frac{\ell}{c}-\frac{r_2}{c}\right)}{D} \end{array} \right] \quad (8)$$

where the geometric impedance factor f_g is the ratio of the antenna input impedance Z_c to the characteristic impedance of free space Z_0 , or $f_g = (Z_c/Z_0)$. It is noted that for a paraboloidal reflector,

$$\frac{\sin(\beta)}{1+\cos(\beta)} = \frac{D}{4F} \quad (9)$$

Our field computations are shown plotted in Figure 10.

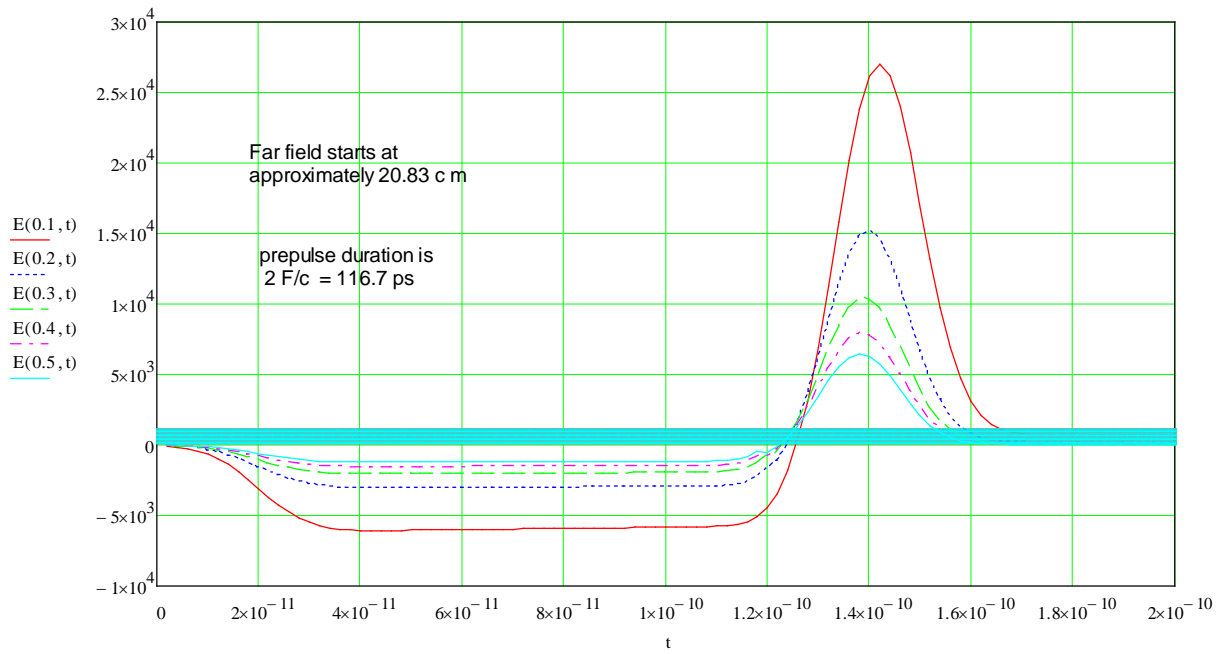


Figure 10. On axis, vertical electric field at distances of 10cm, 20 cm, 30 cm, 40 cm and 50 cm

The magnitude spectra corresponding to the above temporal calculations are shown in Figure 11.

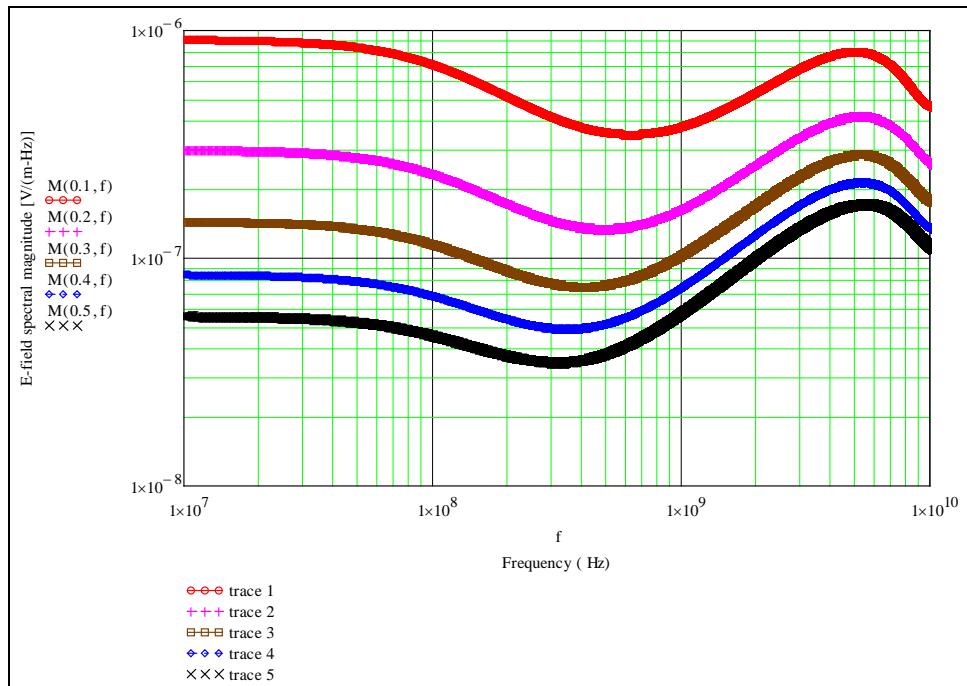


Figure 11. Magnitude spectra of the on-axis vertical electric field

From the field computations shown and unshown above, we can get the field quantities listed in Table 1.

Table 1. Summary of Boresight Vertical electric field (peak values)

#	Boresight Distance r	E_{peak} kV/m	$V_p = r E_{\text{peak}}$ kV	V_p / V_0 with $V_0 = 2$ kV
01	5 cm	40	2.00	1.00
02	10 cm	27	2.70	1.35
03	20 cm	15.3	3.06	1.53
04	30 cm	10.5	3.15	1.58
05	40 cm	8.0	3.20	1.62
06	50 cm	6.5	3.25	1.62
07	60 cm	5.4	3.24	1.62
08	70 cm	4.65	3.25	1.62
09	80 cm	4.07	3.25	1.62
10	90 cm	3.62	3.25	1.62
11	100 cm	3.25	3.25	1.62

As stated earlier, we can conclude that at a boresight distance of about 30 cm, we are already in the far field zone for MIRA.

4. *Fabricational Considerations*

There are many fabricational challenges in building such a small IRA. Previously we have fabricated a 10 cm diameter IRA. These challenges include and are not limited to finding micro-coaxial cables of 100 Ohm impedance and feed point issues of maintain the fields at the feed point and avoid arcing. However, these considerations will come to the forefront only during fabrication and testing and need to be overcome. The pulse output is into an SMA connector of 50 Ohm characteristic impedance. Since a differential output is needed to drive a full IRA like the MIRA, we will need a transmission line balun that transforms the 50 Ohm impedance to the required 200 Ohm impedance at the antenna terminal. The balun is matched to the 50 Ohm source at one end and the 200 Ohm antenna at the antenna terminal. This is shown in Figure 12.

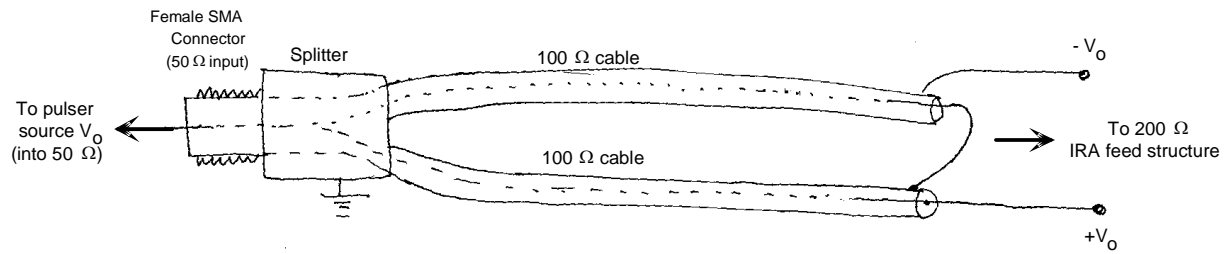


Figure 12. Details of the 50 Ohm to 200 Ohm balun connecting the pulser source to the IRA feed structure.

Figure 13 shows a side view of one of the feed arms. The feed arms come to a point at the feed point and connect to the center conductor of the impedance transformer. It is noted that in Figure 13 we are showing just the top half of the antenna, and we are designing a full IRA.

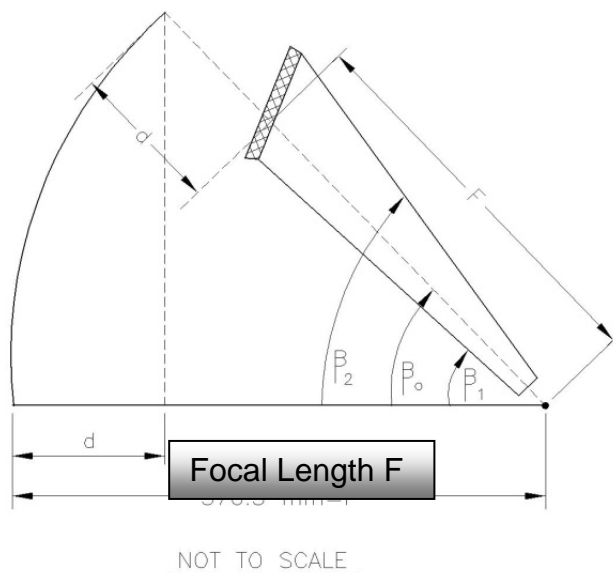


Figure 13. Side view showing the upper flat-plate feed arm

We note the numerical values to be

$$\begin{aligned}
 \mathbf{D} &= \mathbf{50\ mm} \\
 \mathbf{D / 2} &= \mathbf{25\ mm} \\
 \mathbf{F} &= \mathbf{17.5\ mm} \\
 \mathbf{F/D} &= \mathbf{0.35} \\
 \mathbf{d} &= \mathbf{[D^2 / (16 F)] = 8.93\ mm} \\
 \mathbf{(F + d)} &= \mathbf{26.43\ mm} \\
 \mathbf{(F - d)} &= \mathbf{8.57\ mm}
 \end{aligned}
 \tag{10}$$

Note that there are two launcher plates and they are imaged in the ground plane.

Each launcher plate along with its image is a transmission line with 200 Ohm impedance. The two lines are in parallel for a net impedance of 100 Ohms, which matches the impedance transformer.

$$Z_c = \text{Antenna impedance} = 200\ \Omega \text{ (1 launcher plate above ground)}$$

$$Z_c = \frac{Z_o}{2} \frac{K(m)}{K(m_1)} = 60\ \pi \frac{K(m)}{K(m_1)} = 200\ \Omega$$

$$\text{Solving for } m; \quad \rightarrow \quad m = 0.559 \quad m_1 = (1 - m) = 0.440 \tag{10}$$

$$K(m) = \int_0^{\pi/2} \frac{1}{\sqrt{1 - m \sin^2(\theta)}} d\theta \quad K(m_1) = \int_0^{\pi/2} \frac{1}{\sqrt{1 - m_1 \sin^2(\theta)}} d\theta$$

$$\beta_1 = 2 \arctan \left[m^{1/4} \tan \frac{\beta_o}{2} \right] = 63.41^\circ$$

$$\beta_o = \arctan \left[\frac{D}{2(F - d)} \right] = 71.07^\circ$$

$$\beta_2 = 2 \arctan \left[m^{-1/4} \tan \frac{\beta_o}{2} \right] = 78.95^\circ$$

(11)

$$(\beta_2 - \beta_0) = 7.88 \text{ degrees}$$

$$(\beta_0 - \beta_1) = 7.66 \text{ degrees}$$

It is observed that the line denoting the angle β_0 intersects the rim of the reflector.

It is not exactly, but very close to the bisection of angles β_2 and β_1 . Another view of the launcher plates in relation to the reflector is shown in Figure 14. Once again, we are showing only the top half of the full IRA in Figure 14.

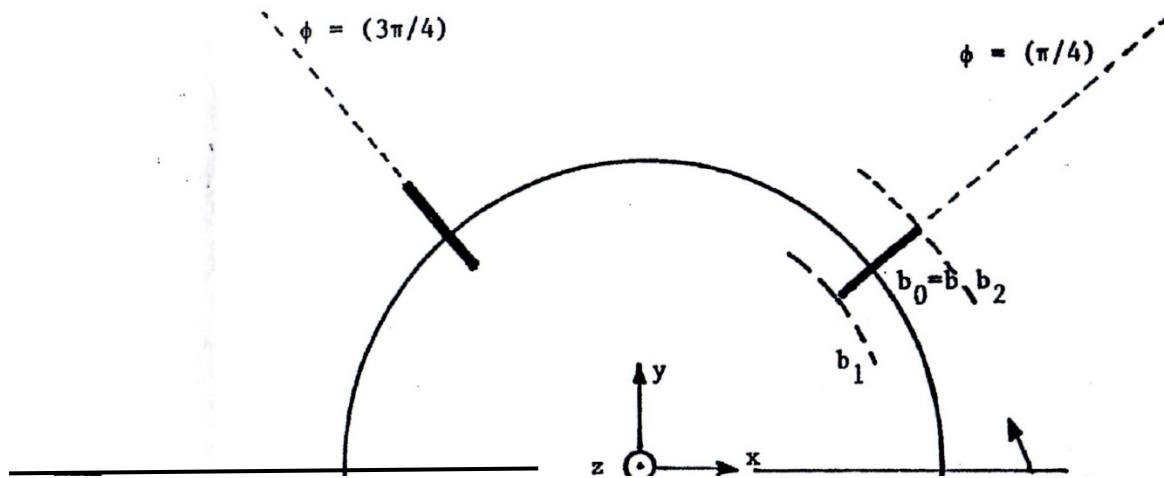


Figure 14. End view of launcher plates and the half reflector

The launcher plates are seen in Figure 14, oriented in such a way that the blockage from them is minimized. In Figure 12, b_1 , b_0 and b_2 are the radii of the edges and the center of the launcher plates, corresponding to the angles β_1 , β_0 and β_2 respectively. These radii are given by

$$b_0 = \frac{D}{2} = \sqrt{b_1 b_2} = 25 \text{ mm}$$

$$b_1 = b_0 m^{1/4} = 21.62 \text{ mm}$$

$$b_2 = b_0 m^{-1/4} = 28.94 \text{ mm}$$

(12)

The calculations shown above are useful in the fabrication of the 5 cm MIRA.

Next we turn our attention to the details of fabricating the launcher plates.

The detail of the feed plates is shown in Figure 15.

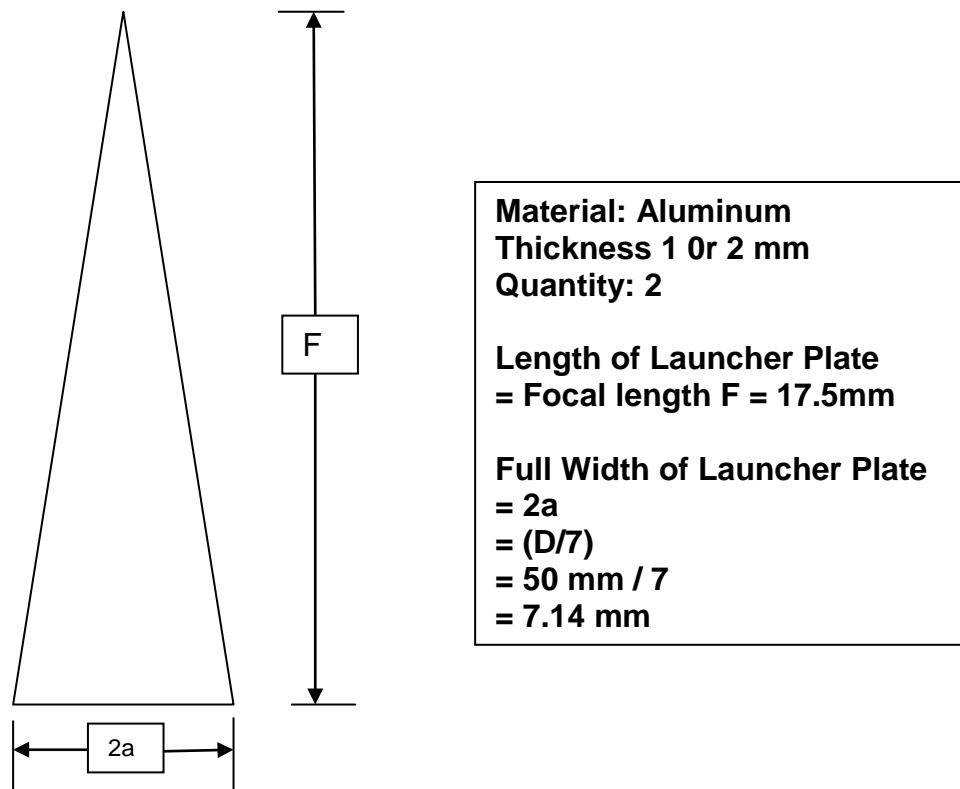


Figure 15. Launcher plate geometry

The dimensions and the material of the launcher plates are also shown in Figure 15.

The length of the launcher plate in Figure 15 is seen to be set equal to the focal length of the reflector. The reason for this is as follows. If the launcher plate is of length F , then the reflection from the end of the launcher plate (if any) will come at exactly the time when the large impulse occurs and the minor reflection from terminator imperfection occurring at the same time will get swamped out by the large impulse. If the pulser is turned on at time $t = 0$, it takes a time of $t_r =$

(r/c) to reach the observer. In the time interval of $t = t_r$ to $t = t_r + (2F/c)$, there will be some energy that goes away from the focal point to the observer and the effect of the presence of the antenna is not yet seen in this time frame. Call this as “prepulse” and the impulse happens at time $t = t_r + (2F/c)$. The reason why prepulse and impulse are of opposite signs is because the electric field reverses in sign when it hits the metallic reflector. So, the prepulse is seen to be negative lasting for a time $(2F/c)$, when the signal reaches the observer.

$(2F/c)$ for our case is seen to be = $(2 \times 1.75 \text{ cm}) / (3 \times 10^{10} \text{ cm/s}) = 116.67 \text{ ps}$

The negative prepulse at the observer location is seen to last for 116.67 ps. This can also be seen in Figure 10.

We also note from Figure 15 that the full width of the launcher plate where the termination starts is given by $2a = (\text{Diameter } D/7)$. In other words, we have set

$$\text{Diameter} / (\text{full width of the launcher plate}) = (D / (2a)) = (50 \text{ mm} / 7.14 \text{ mm}) = 7 \quad (13)$$

This ratio of 7 is needed to ensure that the impedance of each launcher plate to its image in the ground plane is 400 Ohms [See Table 4.1 on page 22 in 7]. Two such lines in parallel results in net impedance of 200 Ohms for the 5 cm MIRA.

We now turn our attention to the Termination at the end of the launcher plates that interconnects the launcher plate to the reflector, as shown in Figure 14.

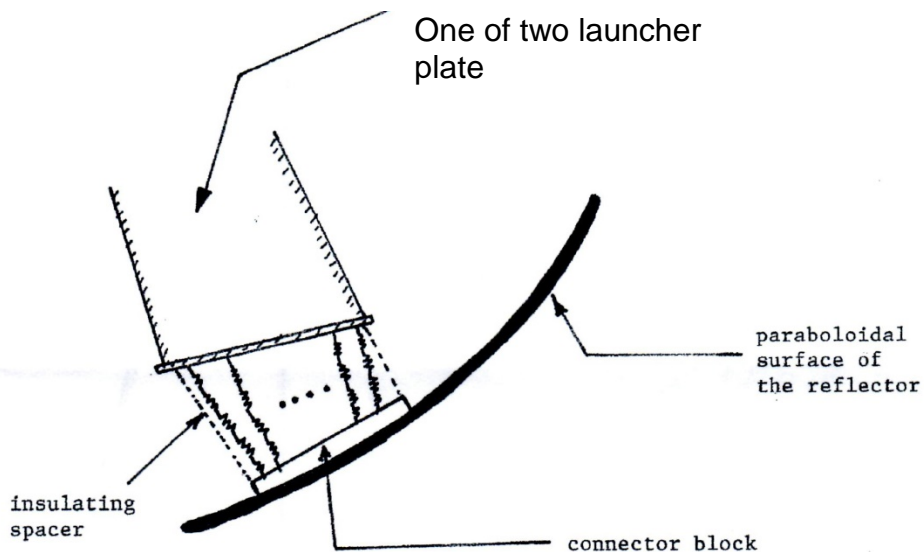


Figure 14. Connecting the launcher plates to the reflector

The net DC resistance of the termination needs to be 200 Ohms. We may use one or more parallel resistors depending on available space in fabrication.

5. *Summary*

In this note, we describe the electromagnetic design considerations of a small (perhaps the world's smallest) or Micro-Impulse Radiating Antenna (MIRA). This author had designed, analyzed, fabricated and tested a 3.66 m diameter IRA (perhaps the world's largest) in 1994 [1-3]. This very first IRA was called the Prototype IRA. We are presenting the design of a Micro-IRA with a diameter of 5 cm for future applications in the areas of detection of hidden objects of cm sizes. At this point, the exclusive interest is in design and analysis of this Micro-IRA. Detailed design and fabrication considerations are presented noting that it will be a challenge to fabricate such a small MIRA.

References

Cited references such as: Sensor and Simulation Notes, Interaction Notes, are available at the URL: <http://ece-research.unm.edu/summa/notes/> and also from the author.

[1]. D. V. Giri, et. al., "A Reflector Antenna for Radiating Impulse-Like Waveforms," Sensor and Simulation Note 382, 4 July 1995.

[2]. D. V. Giri, and C. E. Baum, "Reflector IRA Design and Boresight Temporal Waveforms," Sensor and Simulation Note 365, 2 February 1994.

[3]. D. V. Giri, **High-Power Electromagnetic Radiators: Nonlethal Weapons and Other Applications**, published by Harvard University Press, 2004.

[4]. Picosecond Pulse Labs., now a part of Tektronix. Visit <https://www.tek.com/picosecond-pulse-labs-now-part-tektronix>

[5]. O. V. Mikheev et al., "New Method for Calculating Pulse Radiation from an Antenna with a Reflector", IEEE Transactions on Electromagnetic Compatibility, volume 39, number 1, February 1997, pp 48-54.

[6]. <http://www.fidtechnology.com>

[7]. C. E. Baum, D. V. Giri, and R. D. Gonzalez, Electromagnetic Field Distribution of the TEM Mode in a Symmetrical Two-Parallel-Plate Transmission Line, Sensor and Simulation Note 219, 1 April 1976.